

Article

# Nanosheets of $\text{CuCo}_2\text{O}_4$ As a High-Performance Electrocatalyst in Urea Oxidation

Camila Zequine <sup>1</sup>, Fangzhou Wang <sup>2</sup>, Xianglin Li <sup>2</sup> , Deepa Guragain <sup>3</sup>, S.R. Mishra <sup>3</sup>, K. Siam <sup>1</sup>, P. K. Kahol <sup>4</sup> and Ram K. Gupta <sup>1,5,\*</sup> 

<sup>1</sup> Department of Chemistry, Pittsburg State University, Pittsburg, KS 66762, USA; camilazequine@hotmail.com (C.Z.); ksiam@pittstate.edu (K.S.)

<sup>2</sup> Department of Mechanical Engineering, University of Kansas, Lawrence, KS 66046, USA; fangzhouwang@ku.edu (F.W.); xianglinli@ku.edu (X.L.)

<sup>3</sup> Department of Physics and Materials Science, The University of Memphis, Memphis, TN 38152, USA; ddeepag13@gmail.com (D.G.); srmishra@memphis.edu (S.R.M.)

<sup>4</sup> Department of Physics, Pittsburg State University, Pittsburg, KS 66762, USA; pkahol@pittstate.edu

<sup>5</sup> Kansas Polymer Research Center, Pittsburg State University, Pittsburg, KS 66762, USA

\* Correspondence: ramguptamsu@gmail.com; Tel.: +1-620-2354763

Received: 24 January 2019; Accepted: 20 February 2019; Published: 24 February 2019



**Abstract:** The urea oxidation reaction (UOR) is a possible solution to solve the world's energy crisis. Fuel cells have been used in the UOR to generate hydrogen with a lower potential compared to water splitting, decreasing the costs of energy production. Urea is abundantly present in agricultural waste and in industrial and human wastewater. Besides generating hydrogen, this reaction provides a pathway to eliminate urea, which is a hazard in the environment and to people's health. In this study, nanosheets of  $\text{CuCo}_2\text{O}_4$  grown on nickel foam were synthesized as an electrocatalyst for urea oxidation to generate hydrogen as a green fuel. The synthesized electrocatalyst was characterized using X-ray diffraction, scanning electron microscopy, and X-ray photoelectron spectroscopy. The electroactivity of  $\text{CuCo}_2\text{O}_4$  towards the oxidation of urea in alkaline solution was evaluated using electrochemical measurements. Nanosheets of  $\text{CuCo}_2\text{O}_4$  grown on nickel foam required the potential of 1.36 V in 1 M KOH with 0.33 M urea to deliver a current density of 10 mA/cm<sup>2</sup>. The  $\text{CuCo}_2\text{O}_4$  electrode was electrochemically stable for over 15 h of continuous measurements. The high catalytic activities for the hydrogen evolution reaction make the  $\text{CuCo}_2\text{O}_4$  electrode a bifunctional catalyst and a promising electroactive material for hydrogen production. The two-electrode electrolyzer demanded a potential of 1.45 V, which was 260 mV less than that for the urea-free counterpart. Our study suggests that the  $\text{CuCo}_2\text{O}_4$  electrode can be a promising material as an efficient UOR catalyst for fuel cells to generate hydrogen at a low cost.

**Keywords:** urea oxidation reaction; fuel cells; cyclic voltammetry; hydrogen production

## 1. Introduction

In recent years, the utilization of urea as an alternative fuel in fuel cells has grown significantly, since it is highly available, stable, and nonflammable [1]. Fuel cells are devices that convert chemical energy into electrical energy, playing a vital role in overcoming the world energy crisis [2,3]. Urea is an abundant waste generated in agricultural land, and it is present in industrial and human wastewater as well. Urea is produced from natural gas or can be synthesized from ammonia. When in contact with atmosphere and groundwater, urea breaks down into ammonia and nitrate, causing health and environmental problems [4–6]. A solution to eliminate these problems caused by urea, and to

also generate clean energy, is the urea oxidation reaction (UOR) [7]. This reaction is described as follows [4,5]:



Thermodynamically, water splitting occurs at 1.23 V to generate hydrogen, while urea oxidation could provide hydrogen at a lower potential of 0.37 V [4,8]. This means that urea oxidation provides cheaper hydrogen production than water electrolysis. In previous reports, it is common to see the intense utilization of nickel-based catalysts to oxidize urea efficiently at low overpotential [3,9,10]. Forslund et al. reported a study on the use of  $\text{LaNiO}_3$  as a catalyst for the electrooxidation of urea in alkaline conditions [4]. The nonstoichiometric spinel structure  $\text{Ni}_{1.5}\text{Mn}_{1.5}\text{O}_4$  synthesized by Periyasamy et al., using a hydrothermal synthesis process, showed excellent electrochemical properties with the highest activity toward electro-oxidation of urea in alkaline solutions [1]. The development of porous  $\text{Ni}_3\text{N}$  nanosheet arrays on carbon cloth studied by Liu et al. also showed high performance and was a durable electrocatalyst for urea oxidation [11].

A possibility to use the same principles, but with a different component, led us to develop and produce copper-based catalysts that can oxidize urea efficiently to improve the properties of fuel cells. Electrode materials made of transition metal oxides are often used as electrocatalysts because of their high electrochemical performance, natural abundance, and low cost. In addition, copper and cobalt salts are considered a promising electrode material for energy generation and storage devices due to its nontoxicity and high electrical conductivity. Zheng et al. have shown that cobalt-based compounds are excellent for hydrogen adsorption [12]. Mesostructured  $\text{CuCo}_2\text{S}_4/\text{CuCo}_2\text{O}_4$  nanoflowers were synthesized by Xu et al. and showed an excellent electrochemical performance for energy applications [13]. An asymmetric supercapacitor based on  $\text{CuCo}_2\text{S}_4/\text{CuCo}_2\text{O}_4$  as the cathode and graphene aerogel as the anode delivered a high energy density of 33.2Wh/kg and power density of 13.3 kW/kg. Tong et al. used  $\text{NiMoO}_4$  nanosheets to study the performance in the urea oxidation reaction. They found a larger number of exposed active sites, faster electron transport, and lower adsorption energy of urea molecules. Comparing the cyclic voltammetry (CV) curve recorded in KOH solution, the anodic current density of  $\text{NiMoO}_4$  increased largely after adding urea, demonstrating its high catalytic response activity for electro-oxidation of urea [5]. As reported by Wu et al., a nickel hydroxide electrode with nanocup architecture offered better electrocatalytic performance during electrolysis of urea [14]. Nickel oxide–nickel hybrid nanoarrays on nickel foam ( $\text{NiO-Ni/NF}$ ) was studied by Yue et al. for water splitting and urea oxidation [9]. The electrode showed excellent activity for urea oxidation with the need of a low potential in 1.0 M KOH with 0.33 M urea. Ji et al. reported that open-ended  $\alpha\text{-Ni}(\text{OH})_2$  nanotubes provided effective surface area and active sites when exposed to an electrolyte for urea electrolysis, ensuring a much higher current density during urea electrolysis [15]. Hence, in this work,  $\text{CuCo}_2\text{O}_4$  was synthesized by the hydrothermal method, and the electrocatalytic activity was studied for the oxidation of urea. Materials with three-dimensional (3D) architectures are attractive because their high surface area provides many active sites, and, thus, better electron transfer. The material studied in this report is a 3D flower-like structure composed of  $\text{CuCo}_2\text{O}_4$  nanosheets, which showed excellent electrochemical properties with a high activity.

## 2. Experimental Details

### 2.1. Preparation of $\text{CuCo}_2\text{O}_4$ on Ni Foam

The  $\text{CuCo}_2\text{O}_4$  was synthesized on Ni foam using a one-pot hydrothermal method followed by an annealing process. A piece of Ni foam was cleaned with 3 M HCl solution in an ultrasound bath to remove the NiO layer on the surface, and was then washed with deionized water several times. In a typical synthesis, 528 mg of  $\text{Co}(\text{NO}_3)_2 \cdot 6\text{H}_2\text{O}$ , 93.8 mg of  $\text{Cu}(\text{NO}_3)_2 \cdot 3\text{H}_2\text{O}$ , and 721 mg of urea were dissolved in 34 mL of ethanol. The solution was transferred to a 45 mL Teflon autoclave reactor along with the pre-cleaned Ni foam and maintained at 120 °C for 8 h. After cooling to room temperature, the Ni foam was washed with water and dried under vacuum at 60 °C overnight. Finally, in order to

obtain  $\text{CuCo}_2\text{O}_4$  on the Ni foam, the sample was annealed at  $350\text{ }^\circ\text{C}$  with a temperature ramp rate of  $5\text{ }^\circ\text{C}/\text{min}$  for 2 h in an air atmosphere to obtain  $\text{CuCo}_2\text{O}_4$  (Figure 1).

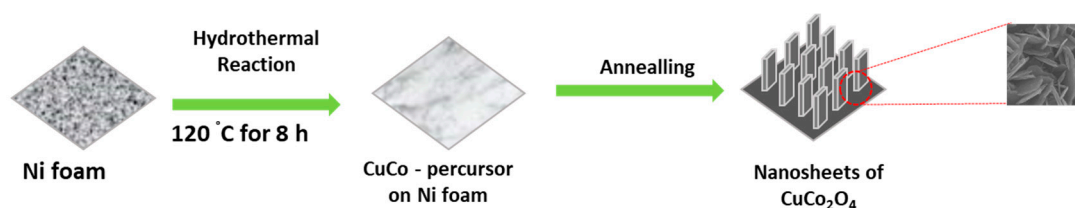


Figure 1. Illustration of the formation of  $\text{CuCo}_2\text{O}_4$  on Ni foam.

## 2.2. Structural Characterization

The structural identity, phase purity, and physical morphology of the fabricated electrode were analyzed using X-ray diffraction (XRD), FEI Versa 3D Dual Beam scanning electron microscopy (SEM), FEI Tecnai F20 XT Field Emission transmission electron microscope (TEM), and Phi 5000 VersaProbe II X-ray photoelectron spectroscopy (XPS).  $\text{CuK}\alpha_1$  ( $\lambda = 1.5406\text{ \AA}$ ) radiation was used to record the X-ray diffraction patterns in  $2\theta$ - $\theta$  mode.

## 2.3. Electrochemical Characterization

To evaluate the catalytic activity of  $\text{CuCo}_2\text{O}_4$  and investigate the function of  $\text{OH}^-$  ions in the electro-oxidation of urea, cyclic voltammetry (CV) was performed in 1 M KOH solution containing 0.33 M urea. These measurements were performed using the standard three-electrode method. A Versastat 4-500 electrochemical workstation (Princeton Applied Research, USA) was used for all electrochemical measurements. A platinum wire and a saturated calomel electrode were used as a counter and a reference electrode, respectively. The synthesized sample on nickel foam was used as the working electrode.

## 3. Results and Discussion

### 3.1. Structural Characterization

X-ray diffraction analysis confirmed a high phase purity of the synthesized  $\text{CuCo}_2\text{O}_4$ , as seen in Figure 2a. All of the diffraction peaks matched well with the JCPDS card no. 78-2177, which corresponded to the pure cubic spinel phase of  $\text{CuCo}_2\text{O}_4$  with a lattice parameter value of  $a = 8.128\text{ \AA}$  [16,17]. Scanning electron microscopy was employed to investigate the sample morphologically. High-magnification SEM images confirmed that  $\text{CuCo}_2\text{O}_4$  was uniformly grown on Ni foam, with a flower-shaped structure composed of nanosheets in different orientations and a smooth surface, revealing a three-dimensional porous structure (Figure 2b). This uniform flower-shaped structure may have been the result of the Faradic reaction. The average diameter of the flower structure was about  $5\text{ }\mu\text{m}$ , and it was interconnected with the nanosheets that had a thickness of 160 nm. TEM images of  $\text{CuCo}_2\text{O}_4$  powder scraped from the Ni foam at various magnifications are shown in Figure 3. TEM images reveal nanorod-like structures with good crystallinity. X-ray photoelectron spectroscopy of the  $\text{CuCo}_2\text{O}_4$  is shown in Figure 3. The XPS survey spectra confirmed the presence of copper, cobalt, oxygen, and carbon elements (Figure 4a). The high-resolution XPS spectrum for Cu 2p showed the existence of  $2p_{1/2}$  and  $2p_{3/2}$  peaks of copper (Figure 4b) [8,18]. The high-resolution XPS spectrum for Co 2p is shown in Figure 4c. The two main peaks of Co  $2p_{3/2}$  and Co  $2p_{1/2}$  were observed around 779.6 and 794.7 eV, respectively, suggesting the existence of both  $\text{Co}^{2+}$  and  $\text{Co}^{3+}$  [8,18]. Considering the Co 2p peak shape, this was consistent with spectra of  $\text{Co}_3\text{O}_4$  standards given by Gu et al. [19] and Yang et al. [20]. These studies showed a  $2p_{3/2}$  peak binding energy of 779.9 eV and a broad plateau-like satellite structure to higher binding energies between the  $2p_{3/2}$  and  $2p_{1/2}$  peaks. The high-resolution spectrum for O 1s is shown in Figure 4d, which shows two peaks centered at 529.4 and 531.3 eV,

respectively. The peak around 529.4 eV corresponded to metal–oxygen bonding, while the second peak corresponded to a high number of defect sites with low oxygen coordination in the material with a small particle size [21].

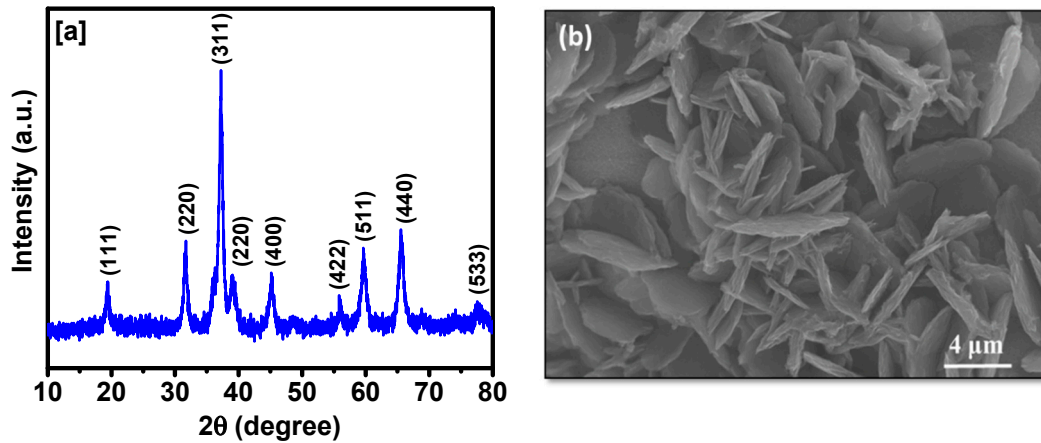


Figure 2. (a) XRD pattern and (b) SEM image of  $\text{CuCo}_2\text{O}_4$ .

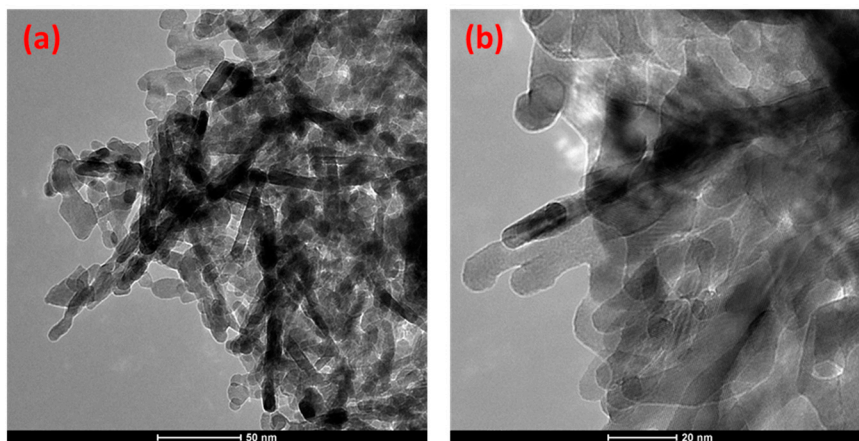


Figure 3. TEM images of  $\text{CuCo}_2\text{O}_4$  at various magnifications.

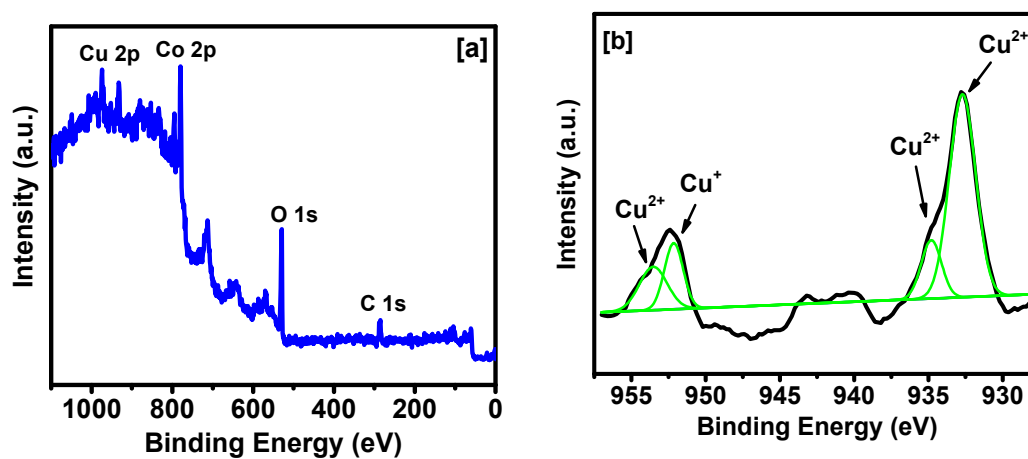
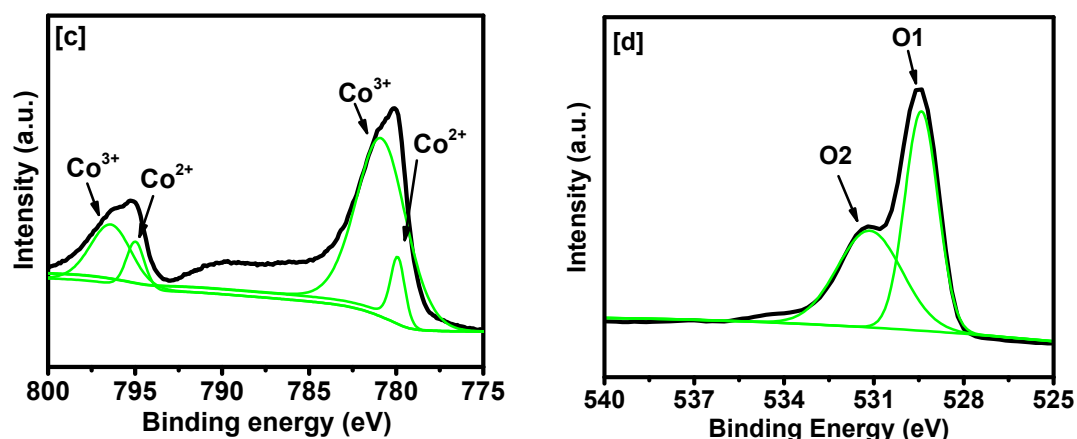


Figure 4. Cont.



**Figure 4.** XPS spectra of the  $\text{CuCo}_2\text{O}_4$ : (a) full survey spectra, (b) Cu 2p spectrum, (c) Co 2p spectrum, and (d) O 1s spectrum.

### 3.2. Electrocatalytic Activities

The electrocatalytic activities of the  $\text{CuCo}_2\text{O}_4$  electrode were examined using a three-electrode setup in 1 M KOH, without and with 0.33 M urea. As seen in Figure 5a, the anodic current density of  $\text{CuCo}_2\text{O}_4$  increased significantly after the addition of urea, confirming a high catalytic activity response of  $\text{CuCo}_2\text{O}_4$  for the electro-oxidation of urea. The  $\text{CuCo}_2\text{O}_4$  electrode demanded a potential of 1.36 V to deliver a current density of  $10 \text{ mA}/\text{cm}^2$ , which was much lower than that without urea. The potential required to deliver  $10 \text{ mA}/\text{cm}^2$  using the  $\text{CuCo}_2\text{O}_4$  electrode was among the more favorable reported values. For example, the  $\text{Ni}(\text{OH})_2$  nanosheet and nanocube required a potential of 1.52 V and 1.55 V, respectively, to produce a current density of  $10 \text{ mA}/\text{cm}^2$  [14,22].  $\text{Ni}_2\text{P}$ , Rhodium-Ni, and NiMo nanosheets demanded a potential 1.37 V, 1.47 V, and 1.37 V, respectively, to generate a current density of  $10 \text{ mA}/\text{cm}^2$  [23–25]. The Tafel slope for the  $\text{CuCo}_2\text{O}_4$  electrode was calculated using polarization data, and was observed to be 82 and 46 mV/dec in 1 M KOH without and with 0.33 M urea, respectively (Figure 5b). The lower Tafel slope in the urea solution indicated faster catalytic kinetic energy for the  $\text{CuCo}_2\text{O}_4$  electrode.

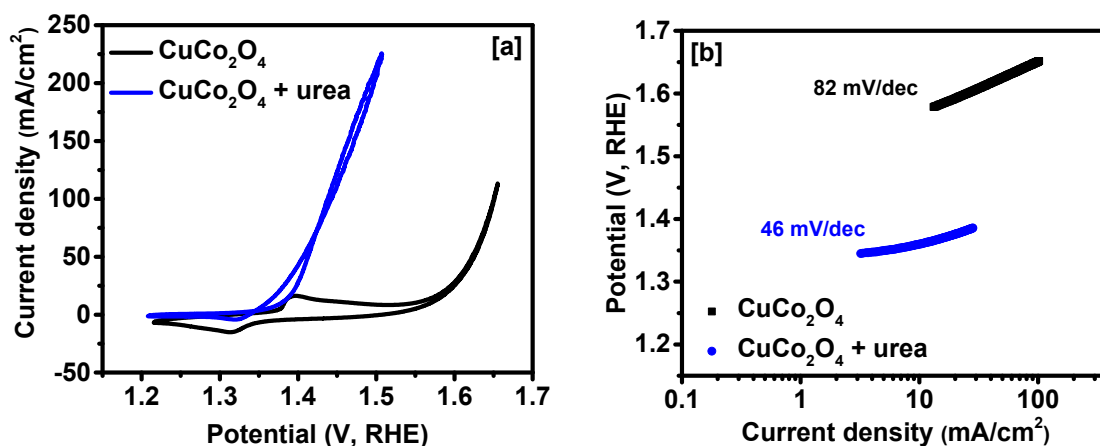


**Figure 5.** (a) Cyclic voltammograms in 1 M KOH with and without 0.33 M urea, and (b) corresponding Tafel slopes.

Furthermore, the urea oxidation kinetics were investigated by electrochemical impedance spectroscopy (EIS). The Nyquist plots for the  $\text{CuCo}_2\text{O}_4$  electrode at various potentials are given in Figure S1. As seen in the Nyquist plots,  $\text{CuCo}_2\text{O}_4$  had a low impedance and, thus, markedly fast kinetics toward urea electro-oxidation. Furthermore, the behavior of the Nyquist plots depended

on the potential. With the increase in the potential, the diameter of the semicircle was decreased, suggesting a lowering in charge transfer resistance. An important method to evaluate the long-term stability of the obtained electrodes in urea oxidation is the chronoamperometric response test. Figure S2 shows the superior catalytic stability with low degradation in current density after 15 h. From this measurement, it was observed that  $\text{CuCo}_2\text{O}_4$  exhibited a stable and durable catalytic performance. The CV curves of the  $\text{CuCo}_2\text{O}_4$  electrode in 1 M KOH electrolyte with 0.33 M urea was measured at various scan rates. Figure S3 shows the variation of measured potential versus scan rates determined using CV data at  $50 \text{ mA/cm}^2$ . As seen in Figure S4, the  $\text{CuCo}_2\text{O}_4$  electrode showed almost no change in potential during CV measurements at various scan rates, indicating superior rate capability for the UOR process. Tests performed by Shi et al. demonstrated an increase in the anodic current density for the Ni/Mo/graphene nanocatalysts after addition of urea in the system [26]. This increase was also found by Barakat et al. in the urea oxidation test for Ni and Mn nanoparticle-decorated carbon nanofibers [27]. Sodium nickel fluoride nanocubes were studied by Kakati et al. in different concentrations of urea for its oxidation [28]. It was found that the peak potentials of urea oxidation increased linearly with increasing urea concentration. Zeng et al. studied the effect in NiCo layered double hydroxide for promoted electrocatalytic urea oxidation, which proved to be efficient, showing a low onset potential and a high faraday efficiency [29].

The electrocatalytic performance of the  $\text{CuCo}_2\text{O}_4$  electrode for hydrogen evolution reaction (HER) was also studied. Figure 6a shows the polarization curves for a  $\text{CuCo}_2\text{O}_4$  electrode in 1 M KOH, without and with 0.33 M urea. As observed, the polarization curves were overlapping each other, indicating the little impact that urea had on the electrochemical activity of the  $\text{CuCo}_2\text{O}_4$  electrode in the HER region. The  $\text{CuCo}_2\text{O}_4$  electrode required a potential of 168 mV to generate  $10 \text{ mA/cm}^2$ . The Tafel slope for the  $\text{CuCo}_2\text{O}_4$  electrode in 1 M KOH without and with urea was observed to be 113 and 112 mV/dec, respectively, suggesting no change in the kinetics for the HER process after addition of urea (Figure 6b). Liu et al. have reported a Tafel slope of 172 and 180 mV/dec for  $\text{Ni}_3\text{N}$  and  $\text{Ni}(\text{OH})_2$  nanosheets on carbon cloth in 1 M KOH + 0.33 M urea solution [11]. The efficiency ( $\eta$ ) for the urea electrolysis can be estimated by the following expression [14]:

$$\eta = \frac{i_t - i_{\text{OER}}}{i_t} \times 100\% \quad (2)$$

where  $i_t$  is the overall current density during electrolysis of urea (1 M KOH + 0.33 M urea) and the  $i_{\text{OER}}$  is the current density of OER process in 1 M KOH at 250 s (Figure S4). An efficiency of 95% was observed for the  $\text{CuCo}_2\text{O}_4$  electrode.

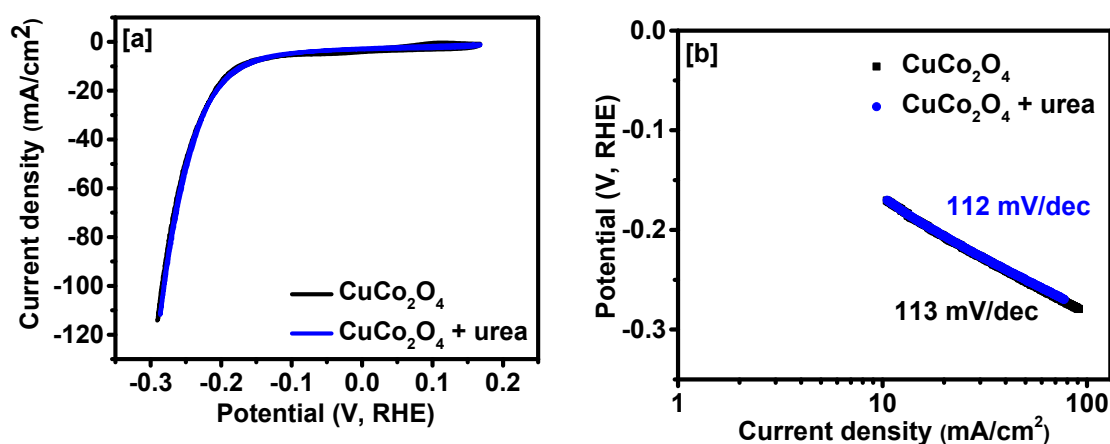


**Figure 6.** (a) Linear sweep voltammetry (LSV) curves of the  $\text{CuCo}_2\text{O}_4$  electrode toward HER in 1.0 M KOH with 0.33 M urea, and (b) corresponding Tafel plots.

The electrocatalytic activities of the  $\text{CuCo}_2\text{O}_4$  electrode were further examined in a two-electrode electrolyzer configuration. The  $\text{CuCo}_2\text{O}_4$  electrode was used as the anode for the UOR and the cathode for the HER process in alkaline media. Figure 7a shows polarization curves of the two-electrode electrolyzer in 1 M KOH, without and with 0.33 M urea. The electrolyzer required a cell voltage of 1.45 V to deliver a current density of 10 mA/cm<sup>2</sup> in urea solution, which was 260 mV less than the cell voltage required without urea in the alkaline solution. The observed cell voltage was better than many other reported systems, such as  $\text{Ni}(\text{OH})_2\text{-Ni}(\text{OH})_2$  and  $\text{Pt/C-RuO}_2$  [11]. In addition, it had a performance in urea solution, and the  $\text{CuCo}_2\text{O}_4$  electrode showed outstanding electrochemical durability (Figure 7b). The chronopotentiometry test, performed for porous pomegranate-like Ni/C in the urea oxidation reaction made by Wang et al., had a stable performance over 12 h [30].

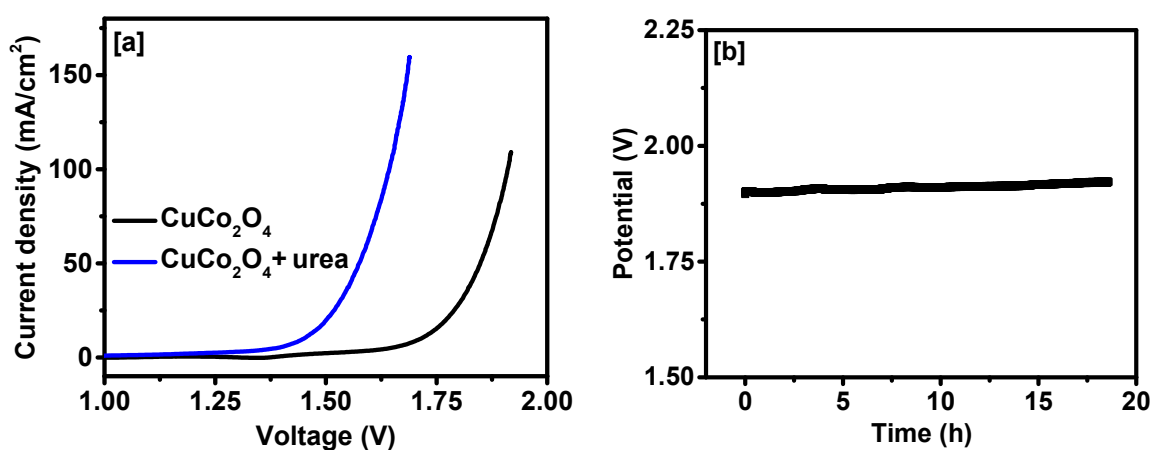


**Figure 7.** (a) Polarization curves for the  $\text{CuCo}_2\text{O}_4$  electrode in 1 M KOH without and with 0.33 M urea, and (b) chronopotentiometric curve for the  $\text{CuCo}_2\text{O}_4$  electrode.

#### 4. Conclusions

In conclusion, it is possible to prove the two main advantages that the urea oxidation reaction can bring to the world: (1) it is a solution to eliminate the urea from groundwater systems and the environment that are harmful to people, and (2) the production of  $\text{H}_2$  uses less energy and has a lower cost, which helps to solve the energy crisis.  $\text{CuCo}_2\text{O}_4$  grown on nickel foam was successfully synthesized, making it possible to utilize them as a highly efficient UOR electrocatalyst under alkaline conditions. The high surface area favors charge transfer capacity and improves the reaction kinetics. The CV curves clearly show a significant decrease in potential after the addition of urea, which leads to cheaper hydrogen production. The two-electrode electrolyzer need a potential of 1.45 V, which is 260 mV less than that for the urea-free counterpart. From the overall investigation, the results suggest that  $\text{CuCo}_2\text{O}_4$  can be used in fuel cells for low-cost hydrogen generation.

**Supplementary Materials:** The following are available online at <http://www.mdpi.com/2076-3417/9/4/793/s1>, Figure S1: Nyquist plots of  $\text{CuCo}_2\text{O}_4$ , Figure S2: Stability performance of the electrode using chronoamperometry, Figure S3: Potential versus scan rates for  $\text{CuCo}_2\text{O}_4$  electrode, Figure S4: Chronoamperograms of  $\text{CuCo}_2\text{O}_4$  electrode in 1 M KOH without and with 0.33 M urea.

**Author Contributions:** R.K.G. conceived the project, designed the experiments, interpreted the data, and finalized the manuscript. The first draft of the manuscript was written by C.Z. C.Z. performed all the electrochemical measurements. F.W. and X.L. provided SEM images, TEM images, and XPS data. All authors reviewed and commented on the manuscript.

**Acknowledgments:** Ram K. Gupta expresses his sincere acknowledgment to the Polymer Chemistry Program and the Kansas Polymer Research Center, Pittsburg State University for providing financial and research support to complete this project. Xianglin Li wants to thank the funding support from NSF (1833048). S. R. Mishra thanks FIT-DRONES and Biologicistic for the financial support.

**Conflicts of Interest:** The authors declare no conflict of interest.

## References

1. Periyasamy, S.; Subramanian, P.; Levi, E.; Aurbach, D.; Gedanken, A.; Schechter, A. Exceptionally Active and Stable Spinel Nickel Manganese Oxide Electrocatalysts for Urea Oxidation Reaction. *ACS Appl. Mater. Interfaces* **2016**, *8*, 12176. [[CrossRef](#)] [[PubMed](#)]
2. Lan, R.; Tao, S.; Irvine, J.T.S. A Direct Urea Fuel Cell—Power from Fertiliser and Waste. *Energy Environ. Sci.* **2010**, *3*, 438. [[CrossRef](#)]
3. Lan, R.; Tao, S. Preparation of Nano-Sized Nickel as Anode Catalyst for Direct Urea and Urine Fuel Cells. *J. Power Sources* **2011**, *196*, 5021. [[CrossRef](#)]
4. Forslund, R.P.; Mefford, J.T.; Hardin, W.G.; Alexander, C.T.; Johnston, K.P.; Stevenson, K.J. Nanostructured LaNiO<sub>3</sub> Perovskite Electrocatalyst for Enhanced Urea Oxidation. *ACS Catal.* **2016**, *6*, 5044. [[CrossRef](#)]
5. Tong, Y.; Chen, P.; Zhang, M.; Zhou, T.; Zhang, L.; Chu, W.; Wu, C.; Xie, Y. Oxygen Vacancies Confined in Nickel Molybdenum Oxide Porous Nanosheets for Promoted Electrocatalytic Urea Oxidation. *ACS Catal.* **2018**, *8*, 1. [[CrossRef](#)]
6. Yan, W.; Wang, D.; Botte, G.G. Nickel and Cobalt Bimetallic Hydroxide Catalysts for Urea Electro-Oxidation. *Electrochim. Acta* **2012**, *61*, 25. [[CrossRef](#)]
7. Zhu, X.; Dou, X.; Dai, J.; An, X.; Guo, Y.; Zhang, L.; Tao, S.; Zhao, J.; Chu, W.; Zeng, X.C.; et al. Metallic Nickel Hydroxide Nanosheets Give Superior Electrocatalytic Oxidation of Urea for Fuel Cells. *Angew. Chem. Int. Ed.* **2016**, *55*, 12465. [[CrossRef](#)] [[PubMed](#)]
8. Yue, Z.; Zhu, W.; Li, Y.; Wei, Z.; Hu, N.; Suo, Y.; Wang, J. Surface Engineering of a Nickel Oxide-Nickel Hybrid Nanoarray as a Versatile Catalyst for Both Superior Water and Urea Oxidation. *Inorg. Chem.* **2018**, *57*, 4693. [[CrossRef](#)] [[PubMed](#)]
9. Boggs, B.K.; King, R.L.; Botte, G.G. Urea Electrolysis: Direct Hydrogen Production from Urine. *Chem. Commun.* **2009**, 4859–4861. [[CrossRef](#)] [[PubMed](#)]
10. Xu, W.; Wu, Z.; Tao, S. Urea-Based Fuel Cells and Electrocatalysts for Urea Oxidation. *Energy Technol.* **2016**, *4*, 1329. [[CrossRef](#)]
11. Liu, Q.; Xie, L.; Qu, F.; Liu, Z.; Du, G.; Asiri, A.M.; Sun, X. A Porous Ni<sub>3</sub>N Nanosheet Array as a High-Performance Non-Noble-Metal Catalyst for Urea-Assisted Electrochemical Hydrogen Production. *Inorg. Chem. Front.* **2017**, *4*, 1120. [[CrossRef](#)]
12. Zheng, Y.; Jiao, Y.; Jaroniec, M.; Qiao, S.Z. Advancing the Electrochemistry of the Hydrogen-Evolution Reaction through Combining Experiment. *Angew. Chem. Int. Ed.* **2015**, *54*, 52. [[CrossRef](#)] [[PubMed](#)]
13. Xu, X.; Liu, Y.; Dong, P.; Ajayan, P.M.; Shen, J.; Ye, M. Mesostructured CuCo<sub>2</sub>S<sub>4</sub>/CuCo<sub>2</sub>O<sub>4</sub> Nanoflowers as Advanced Electrodes for Asymmetric Supercapacitors. *J. Power Sources* **2018**, *400*, 96. [[CrossRef](#)]
14. Wu, M.S.; Ji, R.Y.; Zheng, Y.R. Nickel Hydroxide Electrode with a Monolayer of Nanocup Arrays as an Effective Electrocatalyst for Enhanced Electrolysis of Urea. *Electrochim. Acta* **2014**, *144*, 194. [[CrossRef](#)]
15. Ji, R.Y.; Chan, D.S.; Jow, J.J.; Wu, M.S. Formation of Open-Ended Nickel Hydroxide Nanotubes on Three-Dimensional Nickel Framework for Enhanced Urea Electrolysis. *Electrochem. Commun.* **2013**, *29*, 21. [[CrossRef](#)]
16. Jadhav, H.S.; Pawar, S.M.; Jadhav, A.H.; Thorat, G.M.; Seo, J.G. Hierarchical Mesoporous 3D Flower-like CuCo<sub>2</sub>O<sub>4</sub>/NF for High-Performance Electrochemical Energy Storage. *Sci. Rep.* **2016**, *6*, 31120. [[CrossRef](#)] [[PubMed](#)]
17. Settanni, G.; Zhou, J.; Suo, T.; Schöttler, S.; Landfester, K.; Schmid, F.; Mailänder, V. Protein Corona Composition of PEGylated Nanoparticles Correlates Strongly with Amino Acid Composition of Protein Surface. *arXiv*, **2016**, arXiv:1612.08814.
18. Zhu, J.; Gao, Q. Mesoporous MCo<sub>2</sub>O<sub>4</sub> (M = Cu, Mn and Ni) Spinel: Structural Replication, Characterization and Catalytic Application in CO Oxidation. *Microporous Mesoporous Mater.* **2009**, *124*, 144. [[CrossRef](#)]
19. Gu, D.; Jia, C.-J.; Weidenthaler, C.; Bongard, H.-J.; Spliethoff, B.; Schmidt, W.; Schüth, F. Highly Ordered Mesoporous Cobalt-Containing Oxides: Structure, Catalytic Properties, and Active Sites in Oxidation of Carbon Monoxide. *J. Am. Chem. Soc.* **2015**, *137*, 11407. [[CrossRef](#)] [[PubMed](#)]
20. Yang, J.; Liu, H.; Martens, W.N.; Frost, R.L. Synthesis and Characterization of Cobalt Hydroxide, Cobalt Oxyhydroxide, and Cobalt Oxide Nanodiscs. *J. Phys. Chem. C* **2010**, *114*, 111. [[CrossRef](#)]
21. Wang, J.; Fan, S.; Luan, Y.; Tang, J.; Jin, Z.; Yang, M.; Lu, Y. Ultrathin Mesoporous NiCo<sub>2</sub>O<sub>4</sub> Nanosheets as an Efficient and Reusable Catalyst for Benzylic Oxidation. *RSC Adv.* **2015**, *5*, 2405. [[CrossRef](#)]



22. Wang, D.; Yan, W.; Botte, G.G. Exfoliated Nickel Hydroxide Nanosheets for Urea Electrolysis. *Electrochem. Commun.* **2011**, *13*, 1135. [[CrossRef](#)]
23. Liu, D.; Liu, T.; Zhang, L.; Qu, F.; Du, G.; Asiri, A.M.; Sun, X. High-Performance Urea Electrolysis towards Less Energy-Intensive Electrochemical Hydrogen Production Using a Bifunctional Catalyst Electrode. *J. Mater. Chem. A* **2017**, *5*, 3208. [[CrossRef](#)]
24. Miller, A.T.; Hassler, B.L.; Botte, G.G. Rhodium Electrodeposition on Nickel Electrodes Used for Urea Electrolysis. *J. Appl. Electrochem.* **2012**, *42*, 925. [[CrossRef](#)]
25. Liang, Y.; Liu, Q.; Asiri, A.M.; Sun, X. Enhanced Electrooxidation of Urea Using NiMoO<sub>4</sub>·xH<sub>2</sub>O Nanosheet Arrays on Ni Foam as Anode. *Electrochim. Acta* **2015**, *153*, 456. [[CrossRef](#)]
26. Shi, W.; Ding, R.; Li, X.; Xu, Q.; Liu, E. Enhanced Performance and Electrocatalytic Kinetics of Ni-Mo/Graphene Nanocatalysts towards Alkaline Urea Oxidation Reaction. *Electrochim. Acta* **2017**, *242*, 247. [[CrossRef](#)]
27. Al-deyab, S.S. Ni & Mn Nanoparticles-Decorated Carbon Nanofibers as Effective Electrocatalyst for Urea Oxidation Applied Catalysis A: General. *Appl. Catal. A Gen.* **2015**, *510*, 180.
28. Kakati, N.; Maiti, J.; Lee, K.S.; Viswanathan, B.; Yoon, Y.S. Hollow Sodium Nickel Fluoride Nanocubes Deposited MWCNT as An Efficient Electrocatalyst for Urea Oxidation. *Electrochim. Acta* **2017**, *240*, 175. [[CrossRef](#)]
29. Zeng, M.; Wu, J.; Li, Z.; Wu, H.; Wang, J.; Wang, H.; He, L.; Yang, X. Interlayer Effect in NiCo Layered Double Hydroxide for Promoted Electrocatalytic Urea Oxidation. *ACS Sustain. Chem. Eng.* **2019**, in press. [[CrossRef](#)]
30. Wang, L.; Ren, L.; Wang, X.; Feng, X.; Zhou, J.; Wang, B. Multivariate MOF-Templated Pomegranate-Like Ni/C as Efficient Bifunctional Electrocatalyst for Hydrogen Evolution and Urea Oxidation. *ACS Appl. Mater. Interfaces* **2018**, *10*, 4750. [[CrossRef](#)] [[PubMed](#)]



© 2019 by the authors. Licensee MDPI, Basel, Switzerland. This article is an open access article distributed under the terms and conditions of the Creative Commons Attribution (CC BY) license (<http://creativecommons.org/licenses/by/4.0/>).